the plant journal

SEB SOCIETY FOR EXPERIMENTAL BIOLOGY

The Plant Journal (2024) **119**, 2363–2374 doi: 10.1111/tpj.16922

Molecular basis of one-step methyl anthranilate biosynthesis in grapes, sweet orange, and maize

Michael A. Fallon[1,†], Hisham Tadfie[1,†], Aracely P. Watson[1,†], Madeline M. Dyke[1], Christopher Flores[1], Nathan Cook[2], Zhangjun Fei[3] and Cynthia K. Holland[1,*]

[1]*Department of Biology, Williams College, Williamstown, Massachusetts 01267, USA,*

[2]*Department of Chemistry, Williams College, Williamstown, Massachusetts 01267, USA, and*

[3]*Boyce Thompson Institute, Ithaca, New York 14850, USA*

Received 11 March 2024; accepted 26 June 2024; published online 8 July 2024.

*For correspondence (e-mail ckh2@williams.edu).

†These authors contributed equally.

SUMMARY

Plants synthesize an array of volatile compounds, many of which serve ecological roles in attracting pollinators, deterring herbivores, and communicating with their surroundings. Methyl anthranilate (MeAA) is an anti-herbivory defensive volatile responsible for grape aroma that is emitted by several agriculturally relevant plants, including citrus, grapes, and maize. Unlike maize, which uses a one-step anthranilate methyltransferase (AAMT), grapes have been thought to use a two-step pathway for MeAA biosynthesis. By mining available transcriptomics data, we identified two AAMTs in *Vitis vinifera* (wine grape), as well as one ortholog in "Concord" grape. Many angiosperms methylate the plant hormone salicylic acid (SA) to produce methyl salicylate, which acts as a plant-to-plant communication molecule. Because the *Citrus sinensis* (sweet orange) SA methyltransferase can methylate both anthranilate (AA) and SA, we used this enzyme to examine the molecular basis of AA activity by introducing rational mutations, which identified several active site residues that increase activity with AA. Reversing this approach, we introduced mutations that imparted activity with SA in the maize AAMT, which uncovered different active site residues from those in the citrus enzyme. Sequence and phylogenetic analysis revealed that one of the *Vitis* AAMTs shares an ancestor with jasmonic acid methyltransferases, similar to the AAMT from strawberry (*Fragaria* sp.). Collectively, these data demonstrate the molecular mechanisms underpinning AA activity across methyltransferases and identify one-step enzymes by which grapes synthesize MeAA.

Keywords: biochemistry, wine grapes (*Vitis vinifera*), "Concord" grapes, sweet orange (*Citrus sinensis*), maize (*Zea mays*), methyltransferase, methyl anthranilate, methyl salicylate, enzyme function.

INTRODUCTION

Plants synthesize an array of volatiles that impart distinct aromas (Dudareva et al., 2004, 2006). These volatiles serve biological and ecological roles that enable plants to attract pollinators and seed dispersers, repel herbivores, and communicate with their surroundings, including other plants (Schuman, 2023). Plant volatiles also have economic value as aromatic and flavoring agents in the food, beverage, cosmetic, fragrance, and pharmaceutical industries (Baldwin, 2010). Many flowering plants synthesize the wintergreen aroma compound methyl salicylate (MeSA), which is the methyl ester of the plant hormone salicylic acid (SA) (Figure 1) (Effmert et al., 2005). Methyl anthranilate (MeAA) is the methyl ester of the tryptophan pathway intermediate anthranilate (AA) and is responsible for the recognizable aroma of grapes (Li et al., 2023; Wang & De Luca, 2005). In addition to being volatiles, methylating plant hormones, such as SA, jasmonate, and indole 3-acetic acid (auxin), inactivates them and modulates their activities (Westfall et al., 2013).

Methyl anthranilate-producing species include many agriculturally relevant crops, such as maize (*Zea mays*), alfalfa (*Medicago truncatula*), fox grapes (*Vitis labrusca*), strawberries (*Fragaria* spp.), citrus (*Citrus* spp.), and soybeans (*Glycine max*) (Gonzalez-Mas et al., 2019; Kollner et al., 2010; Lin et al., 2013; Pillet et al., 2017; Pollier et al., 2019; Wang & De Luca, 2005). MeSA and MeAA play important roles in plant defense against herbivores. When plants are under attack by aphids, they emit volatile MeSA, which can travel long distances to neighboring plants that perceive MeSA, demethylate it, and use the resulting SA to regulate transcriptional responses and

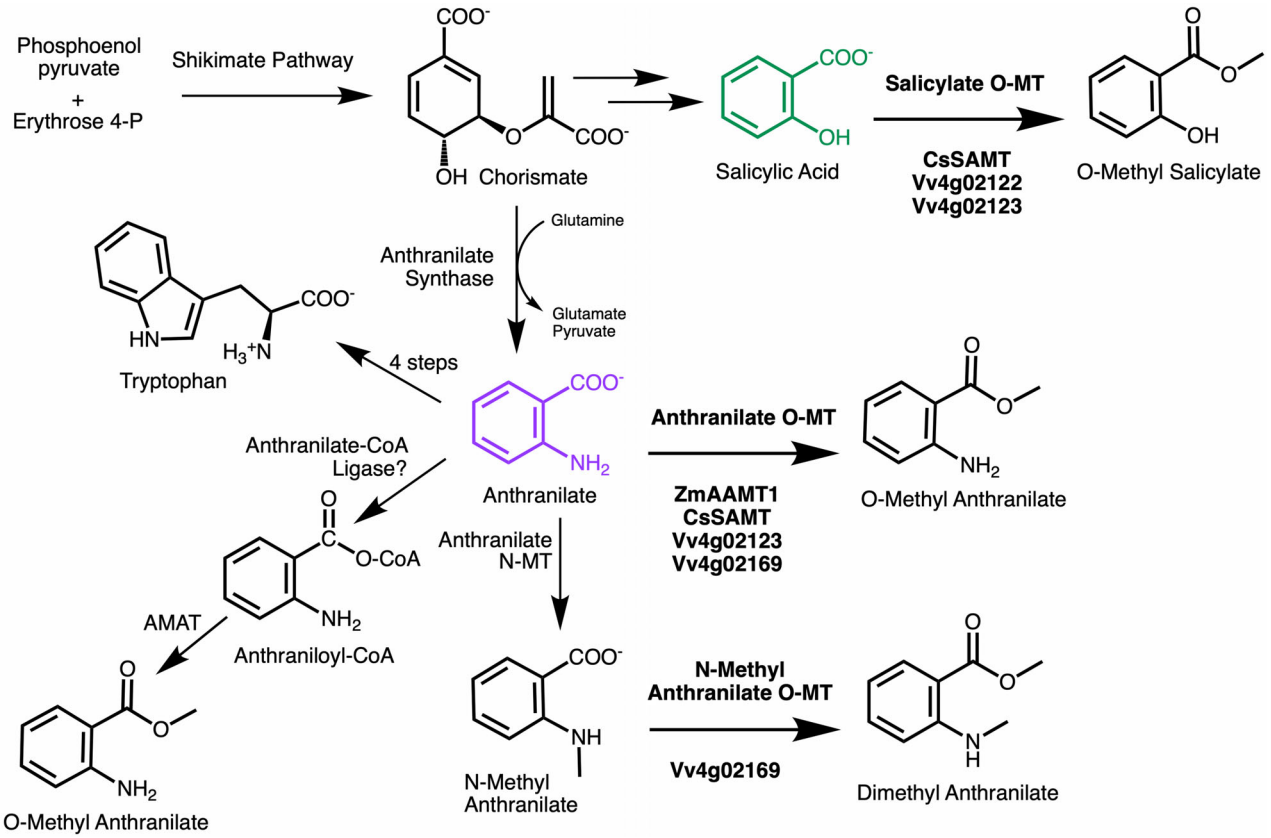

Figure 1. Schematic diagram of the biosynthesis and fates of anthranilate in plants. The names of enzymes investigated here in citrus (Cs), grapes (Vv), and maize (Zm) are displayed in bold below the arrow.

elicit defenses (Gong et al., 2023). Citrus plants that are infected with the psyllid-vectored bacterial pathogen *Candidatus* Liberibacter asiaticus (CLas), the causal agent of citrus greening (huanglongbing), release high levels of MeSA, while uninfected plants release high levels of MeAA (Mann et al., 2012). MeSA, but not MeAA, attracts the psyllid (*Diaphorina citri*) to the plant, which in turn may promote the spread of the pathogen. Strawberries that are resistant to *Drosophila suzukii* pest flies produce high concentrations of MeAA, which attracts the egg-laying adults but then leads to reduced hatching rates of their eggs (Bracker et al., 2020). Maize synthesizes and releases a volatile blend that contains MeSA and MeAA in response to insect damage, which then attracts wasps that parasitize the insect herbivores (Turlings et al., 1990; von Merey et al., 2013). Exogenous application of MeAA on crops has also been shown to be effective in attracting natural enemies of herbivores to protect plants from further damage (Simpson et al., 2011). Commercially, MeAA is also an effective bird repellant, and MeAA sprays are available for deterring birds from orchards and turf (Avery et al., 1995; Mason et al., 1989; Mikiciuk et al., 2021).

Although humans frequently associate the aroma of MeAA with grapes, the biosynthetic pathway has remained incomplete in *Vitis* spp. (Wang & De Luca, 2005). While MeAA is high in "Concord" grape juices, this compound contributes to a "foxy" aroma that is undesirable in wine and is found at low or undetectable levels in wine grapes (*Vitis vinifera*) (Lin et al., 2019; Sun et al., 2011). In "Washington Concord" grape, an anthraniloyl-coenzyme A (CoA): methanol acyltransferase (AMAT) that condenses anthraniloyl-CoA and methanol into MeAA has been identified (Figure 1) (Wang & De Luca, 2005). However, the two-step MeAA pathway remains incomplete as the first pathway enzyme – anthranilate-CoA ligase – remains to be discovered.

Maize and strawberry instead use a one-step S-adenosyl-L-methionine (SAM)-dependent methyltransferase for MeAA biosynthesis (Kollner et al., 2010; Pillet et al., 2017), and in citrus, a one-step salicylic acid methyltransferase (SAMT) that can methylate AA has been identified (Huang et al., 2016) (Figure 1). *SAMT* orthologs are found in most angiosperm orders (Dubs et al., 2022), and while MeAA has been detected in the headspace floral volatiles of at least 19 plant families (Knudsen et al., 2006),

AA-using enzymes remain largely unidentified in MeAA-producing plants. Because SA and AA are structurally similar and differ only in that the *ortho* hydroxyl on SA is an amine on AA, we hypothesized that active site residues in SA- and/or AA-using methyltransferase would confer activity with and specificity for one or both substrates. We first sought to identify and functionally characterize anthranilate methyltransferases (AAMTs) in grapes (*Vitis* spp.) by mining available metabolomics, transcriptomics, and genomic resources. Furthermore, we set out to trace the molecular mechanisms of AA recognition in SABATH (*s*alicylic *a*cid MT, *b*enzoic *a*cid MT, *th*eobromine synthase) methyltransferases in citrus and maize.

RESULTS AND DISCUSSION

Identification of one-step SAM-dependent AAMTs in grapes

While citrus, maize, and strawberries synthesize MeAA using a one-step methyltransferase, *Vitis* spp. are thought to synthesize MeAA via a two-step two-enzyme pathway, and only the second enzyme in this pathway, an AMAT, has been characterized (Wang & De Luca, 2005) (Figure 1). AMAT had a turnover rate of 1.32 min^{-1} and displayed 26-fold higher relative activity with benzyl alcohol compared to methanol, suggesting that additional enzymes may be responsible for MeAA synthesis in grapes (Wang & De Luca, 2005). Although the *AMAT* gene expression profile corresponds to MeAA levels in berries during ripening (Yang et al., 2020), we hypothesized that grapes may also have a SABATH methyltransferase that could catalyze the methylation of AA. Published metabolomics data showed that MeAA levels increase throughout fruit ripening, and this same study used transcriptomics to identify genes that are expressed in ripening fruits in various *Vitis* wine accessions and in "Concord" (Yang et al., 2020). From these available "omics" data, we selected four candidate methyltransferases that have the highest expression in "Concord" fruit, where MeAA accumulates (Data S1).

To determine whether the four candidate methyltransferases from *V. vinifera* were active with AA, each enzyme was assayed *in vitro*, and this confirmed that two of the candidates from *V. vinifera* (Vv4g02123 and Vv4g02169) methylated AA (Figure 2a). Vv4g02123 had similar activities with 1 mM AA, SA, and BA, but the K_m values could not be captured because the activity was linear to 1 mM, indicating that the enzyme did not have a preference for these substrates (Figure 2b,d; Figure S1). Unexpectedly, when assayed with *N*-methyl AA (*N*-MeAA), Vv4g02123 had a low K_m value of 12 μM, suggesting that the enzyme prefers *N*-MeAA as a substrate, forming dimethyl AA (DiMeAA) (Figure 2a,c). However, Vv4g02123 had a 2-fold lower activity with 1 mM *N*-MeAA compared to its activity with 1 mM AA. The products of Vv4g02123 – MeAA and DiMeAA – were confirmed by gas chromatography–mass spectrometry (GC–MS) in comparison to authentic standards (Figures S2 and S3).

DiMeAA is also volatile, but very little is known about its biosynthesis in plants. Synthesizing DiMeAA would require a pool of *N*-MeAA to use as a substrate, which may be synthesized by an anthranilate *N*-methyltransferase (Figure 1). While an anthranilate *N*-methyltransferase has been identified in common rue (*Ruta graveolens*) (Rohde et al., 2008), one remains to be identified in *Vitis* spp. DiMeAA (also methyl *N*-methyl aminobenzoate) has been reported in floral volatiles of plants in the Orchidaceae and Rutaceae but has yet to be identified in Vitaceae species (Knudsen et al., 2006).

The second candidate that was active with AA, Vv4g02169, had a low K_m value of 160 μM for AA, suggesting that this was the preferred substrate (Figure 2h). Also, Vv4g02169 had a fivefold higher activity with AA compared to BA, and activity was not detected with SA or *N*-MeAA (Figure 2a). We hypothesized that another candidate, Vv4g02122, would function as an AAMT based on high gene expression in "Concord" berries (Yang et al., 2020), but it methylated SA, had minimal activity with AA, and was inactive with BA (Figure 2a; Figure S1). The fourth candidate, Vv12g00725, did not methylate SA, AA, BA, or *N*-MeAA when assayed *in vitro*. Therefore, we have identified two *V. vinifera* enzymes that produce MeAA, and one of which also produces DiMeAA.

While these enzymes were from wine grapes (*V. vinifera*), MeAA is found at low concentrations in wine grapes and at high concentrations in "Concord," which is a hybrid of *V. labrusca* with roughly one-third of its genome from *V. vinifera* (Sawler et al., 2013). Since published transcriptomics data indicates all of the identified methyltransferases are expressed in both *V. vinifera* and "Concord" berries during ripening, we sought to understand the genomic variation that accounts for the differences in their MeAA profiles. To illuminate differences in gene expression and/or enzyme activity, we compared the promoter and gene sequences of the two AA-using methyltransferases, *Vv4g02123* and *Vv4g02169*, to those of *V. labrusca* and "Concord." In the promoter region, there is a 166-bp deletion that is 784 bp upstream of the start codon and a 23-bp insertion that is 686 bp upstream of the start codon in *V. labrusca* and "Concord" orthologs when compared to the promoter of *Vv4g02123* (Figure S4). In the promoter of the "Concord" ortholog of *Vv4g02169*, there is an AT-rich 32-bp insertion 1 kb upstream of the start codon that is not found in either *V. labrusca* or *V. vinifera*, as well as other small insertions and deletions that are not found in either parent (Figure S5). These promoter differences may contribute to differences in gene expression that lead to altered MeAA biosynthesis across grape cultivars.

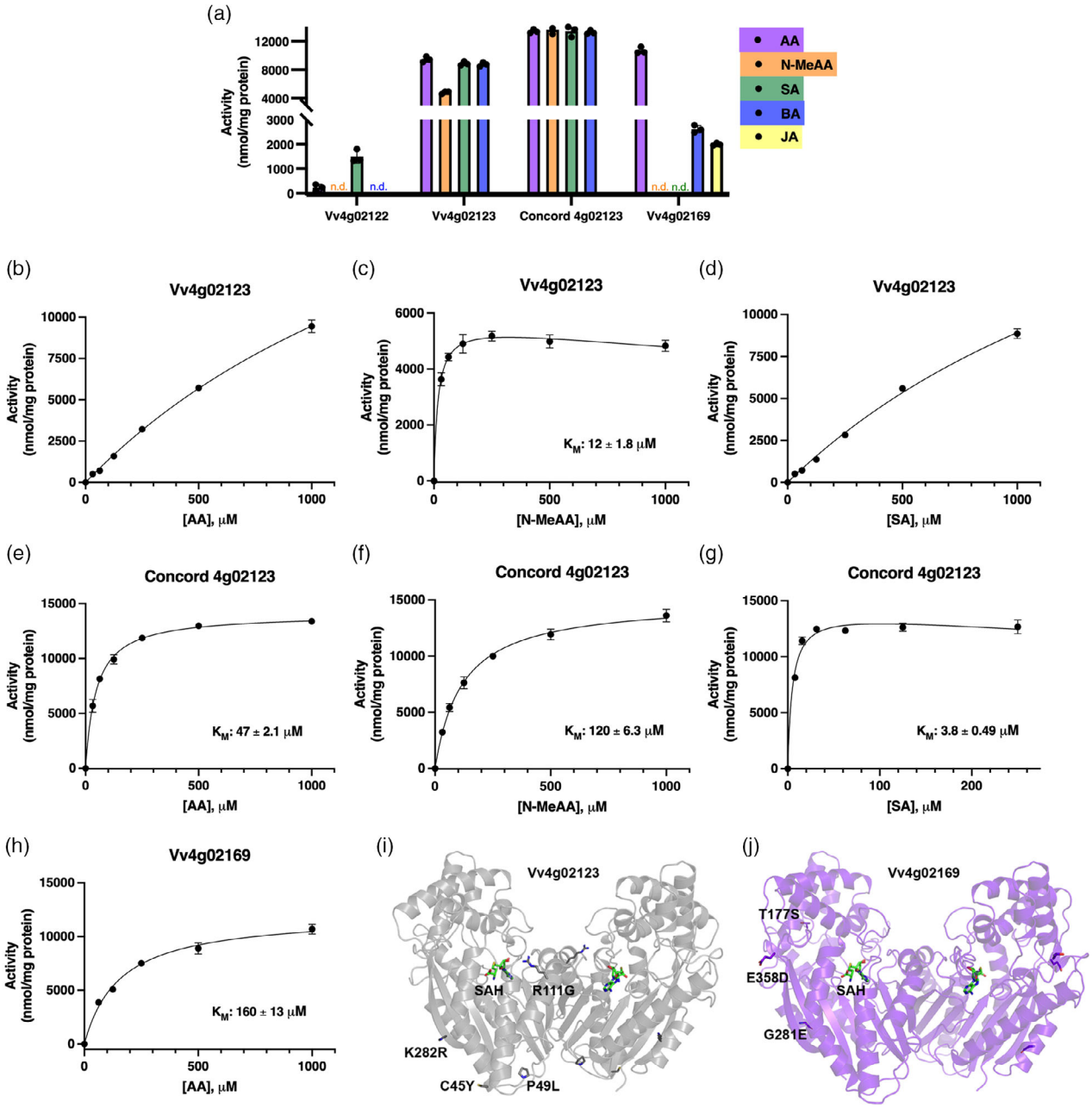

Figure 2. Identification of two anthranilate methyltransferases in *Vitis vinifera* and "Concord."
(a) Enzyme activity across *Vitis vinifera* (Vv) and "Concord" methyltransferases with 1 mM substrates. Only Vv4g2169 was assayed with jasmonic acid (JA).
(b) Kinetics plot of Vv4g02123 with varied anthranilate (AA), (c) varied *N*-methyl anthranilate (*N*-MeAA) fit to a substrate inhibition kinetics curve, and (d) varied salicylic acid (SA).
(e) Kinetics plot of the "Concord" ortholog of Vv4g02123 with varied AA, (f) varied *N*-MeAA, and (g) varied SA, which was fit to a substrate inhibition kinetics curve.
(h) Kinetics plot of Vv4g02169 with varied AA.
(i) Structural differences between Vv4g02123 and (j) Vv4g02169 in *V. vinifera* and their orthologs in "Concord." SAH (green) is positioned in the active site of each dimer. For all points, $n = 3$; where error bars are not visible, the standard deviation is too small to visualize.

In addition to changes in gene expression, mutations in the coding sequence could lead to altered enzyme activity. The coding sequence of the "Concord" ortholog of *Vv4g02123* is conserved in *V. labrusca* but has four single nucleotide differences that cause amino acid changes in comparison to *V. vinifera* (C45Y, P49L, R111G, and K282R) (Figure 2i; Figure S6). Cys45, Pro49, and Lys282 are positioned away from the active site, while Arg111 is located

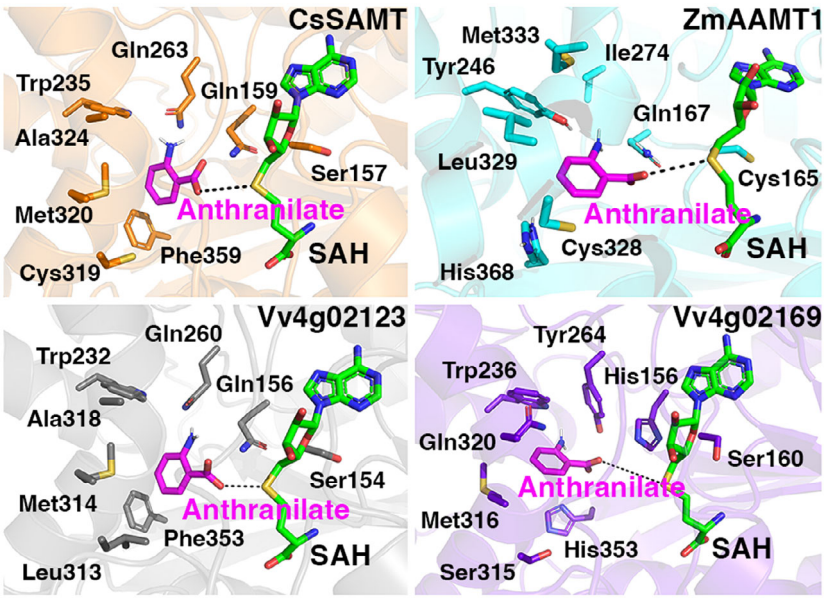

Figure 3. Active site comparisons of four enzymes that generate *O*-methyl anthranilate: *Citrus sinensis* SAMT (CsSAMT), *Zea mays* AAMT1 (ZmAAMT1), *Vitis* Vv4g02123, and *Vitis* Vv4g02169. Anthranilate (magenta) was docked into each active site and SAH (green) was overlaid from a solved structure (PDB: 1M6E).

within a helix at the dimer interface. The "Concord" and *V. labrusca* orthologs of *Vv4g02169* also have conserved coding sequences; however, there is an in-frame three-bp deletion in the *V. labrusca* gene that deletes Lys4 (Figure S7). The *V. vinifera* Vv4g02169 and its "Concord" ortholog differ by three amino acids (T177S, G281E, and E358D) (Figure 2j) that are positioned away from the active site and the dimer interface. While these amino acid differences were outside the active site, we purified and assayed the "Concord" ortholog of 4g02123 and 4g02169 to determine whether this variation would impact activity.

When we assayed the "Concord" ortholog of 4g02123, it retained activity with AA and had a low K_m value of 47 μM, which is greatly reduced in comparison to the *V. vinifera* ortholog (Figure 2e). While the *V. vinifera* ortholog had a very low K_m value with *N*-MeAA, the "Concord" ortholog had a 10-fold increased K_m value of 120 μM with *N*-MeAA, suggesting that the "Concord" enzyme has a relaxed preference for *N*-MeAA (Figure 2f) relative to the *V. vinifera* enzyme (Figure 2c). The lowest K_m value of any substrate with the "Concord" 4g02123 was 3.8 μM with SA, followed by 23 μM with BA (Figure 2g; Figure S2). Although there are only three minor amino acid changes between 4g02169 in *V. vinifera* and "Concord," the "Concord" ortholog was inactive *in vitro*, and MeAA could not be detected in the media from *Escherichia coli* expressing the gene or single mutants of the gene. This was surprising, especially when considering that these three amino acids are positioned outside of the active site and away from the dimer interface (Figure 2j). Therefore, the "Concord" ortholog of 4g02123 likely represents the primary one-step methyltransferase for MeAA biosynthesis, and the 166-bp deletion within 1 kb of the start codon may account for differences in MeAA profiles across grape accessions (Figure S4).

Structure-guided analysis of AA activity in the sweet orange SAMT

Previous efforts to trace the substrate specificity for AA used the maize AAMT1, which found an active site mutation that conferred activity with SA, Y246W (Kollner et al., 2010). Because CsSAMT can methylate SA, AA, and BA and its expression correlates with MeAA presence in citrus flowers (Azam et al., 2013; Huang et al., 2016), we reasoned that this was a good candidate for identifying additional active site residues that contribute to AA recognition and activity in a SAMT. To identify putative active site residues that may be responsible for AA activity, we generated AlphaFold structural models of the CsSAMT and overlaid them with a solved structure of the *Clarkia breweri* SAMT, which had been co-crystalized with S-adenosyl-L-homocysteine (SAH) and SA (Zubieta et al., 2003). Active site residues that varied between functionally characterized AAMTs and methyltransferases that use SA or BA were identified as candidates for site-directed mutagenesis (Figure 3). These comparisons led us to mutate six variable active site residues to examine their role in AA activity: Gln159, Gln263, Cys319, Met320, Ala324, and Phe359 (Table 1).

Mutant enzymes were kinetically characterized to compare their activity profiles and K_m values with AA, SA, and BA to the wild-type CsSAMT (Table 1). While the

Table 1 Activities of CsSAMT wild type and single mutants with salicylic acid, anthranilate, and benzoic acid

	Salicylic acid		Anthranilate		Benzoic acid	
Protein	K_m value ± SE (μM)	Activity with 1 mM ± SD (nmol mg^{-1})	K_m value ± SE (μM)	Activity with 1 mM ± SD (nmol mg^{-1})	K_m value ± SE (μM)	Activity with 1 mM ± SD (nmol mg^{-1})
CsSAMT	105 ± 11	8000 ± 340	n.d.	870 ± 250	n.d.	1900 ± 280
SAMT-Q159H	390 ± 33	3300 ± 250	n.d.	160 ± 51	n.d.	1300 ± 35
SAMT-Q263C	840 ± 78	5800 ± 110	480 ± 75	1600 ± 101	n.d.	480 ± 170
SAMT-Q263Y	480 ± 78	6800 ± 900	230 ± 15	2900 ± 45	n.d.	150 ± 32
SAMT-C319S	180 ± 10	10 300 ± 130	790 ± 190	1500 ± 82	n.d.	760 ± 110
SAMT-M320I	200 ± 10	9400 ± 260	n.d.	1400 ± 110	n.d.	2600 ± 180
SAMT-M320L	560 ± 42	5200 ± 140	n.d.	1200 ± 23	n.d.	310 ± 34
SAMT-A324M	n.d.	5900 ± 260	980 ± 150	1700 ± 94	n.d.	290 ± 49
SAMT-A324T	260 ± 13	9600 ± 240	n.d.	420 ± 120	n.d.	1400 ± 6.4
SAMT-F359H	n.d.	690 ± 150	n.d.	n.d.	n.d.	n.d.

Activities with 1 mM substrates are reported because the data were generated from endpoint assays. $n = 3$ replicates.
n.d., none detected; SD, standard deviation; SE, standard error.

wild-type CsSAMT had a low K_m value of 105 μM for SA, all of the mutant enzymes had increased K_m values relative to the wild type. For the A324M and F359H mutants, activity was linear to 1 mM when SA concentrations were varied, meaning the K_m value had increased to the point where it was unable to be saturated (Figure S8). These increased K_m values suggest that all six residues are essential for SA recognition.

While all of the mutations increased K_m values with SA, we were surprised that three of the mutants, C319S, M320I, and A324T had increased activity with 1 mM SA compared to the wild-type CsSAMT (Table 1). However, mutations at positions Met320 and Ala324 to different residues, Leu and Met, respectively, led to 35% less activity with SA compared to the wild-type enzyme, demonstrating that amino acid substitutions at these positions are key for SA activity. The F359H mutant had very low activity with SA, and the K_m value was also not able to be captured, which indicates that having the aromatic, nonpolar Phe in the CsSAMT active site may be critical for binding aromatic substrates.

When the mutant enzymes were assayed with AA, four of the mutations, Q263C, Q263Y, C319S, and A324M, introduced detectable K_m values when AA was varied (Table 1). The mutations at position 263 led to the lowest K_m values of any of the mutants, 230 and 480 μM, when a tyrosine or cysteine was introduced, respectively. For both of these Gln263 mutants, the K_m value for AA is reduced to almost half that of SA. The C319S mutant still had a lower K_m value for SA (180 μM) than for AA (790 μM). For A324M, the K_m value of 980 μM with AA was high, but AA was the only substrate for which the K_m value was able to be captured for this mutant. Taken together, the lower K_m values for AA relative to other substrates for Q263C, Q263Y, and A324M imply that these two residues (Gln263 and Ala324) are critical for AA recognition in CsSAMT.

Six of the mutations (Q263C, Q263Y, C319S, M320I, M320L, and A324M) increased activity with AA relative to the wild-type enzyme, ranging from 1.4-fold higher activity for the M320L mutant to 3.3-fold higher activity for the Q263Y mutant (Table 1). When we compared the ratio of activity of AA to SA for each of the mutants relative to that of the wild-type CsSAMT, these six mutants also all had increased ratios (Figure S9). The Q263Y mutant had a ratio of AA to SA that was 3.9-fold higher than that of the wild-type enzyme, which represents a substantial shift in preference. The AA to SA ratio for the Q263C and A324M mutants was 2.5-fold higher than that of the wild-type enzyme, highlighting the importance of these two positions for conferring AA activity.

When the mutants were assayed with BA, none of the mutations led to a detectable K_m value (Table 1). Only one mutation, M320I, led to 38% increased activity with BA compared to the wild-type enzyme. Notably, the Q263Y, M320L, and A324M mutants, which had high activity with AA, had 12.7-, 6.1-, and 6.6-fold lower activity with BA, respectively, further emphasizing the role of these positions in AA substrate specificity.

Overall, we have identified three residues in the CsSAMT active site that confer AA activity: Gln263, Cys319, and Ala324. One or more mutations at these positions reduced the K_m value with AA and also increased the ratio of activity with AA to SA relative to the wild-type enzyme (Table 1; Figure S9). While the CsSAMT has high activity with AA, it is possible that additional SABATH methyltransferases that have yet to be characterized may also synthesize MeAA. There may also be an AMAT in *Citrus* spp. that is responsible for generating AA esters using anthraniloyl-CoA and methanol, similar to the enzyme in grapes (Wang & De Luca, 2005; Yang et al., 2020).

Revisiting substrate specificity of the maize AAMT1

Although the maize AAMT1 had already been probed for SA specificity, we wondered whether introducing residues that were found to be critical for substrate recognition in the *Citrus sinensis* SAMT would impart SA activity in ZmAAMT1. To test this, we compared the active site of the ZmAAMT1 enzyme to other SABATH methyltransferases, including the CsSAMT and the grape enzymes, 4g02123 and 4g02169, which were identified in this study (Figure 3). Twelve single mutations were introduced – F164S, F164Y, C165S, Q167W, Y246H, L329M, M333A, M333T, H368F, H368T, and H368Y, as well as the Y246W mutant that was previously shown to introduce activity with SA (Kollner et al., 2010). The resulting mutant proteins were inactive in two *in vitro* assays with the exception of the ZmAAMT1 L329M mutant, which had a 3.8-fold higher AA activity when assayed using ^{14}C-labeled SAM and 25% higher activity when MeAA production was quantified by GC–MS (Figure 4a; Figure S10 and S11). Kollner et al. (2010) had success in assaying Y246W, Q167M, and Q167H mutations in the same enzyme and found that they were active with AA, and the Y246W mutant introduced 13% activity with SA relative to activity with AA. While we did not see activity with these mutants *in vitro*, we did detect MeAA in the media of *E. coli* that were expressing each mutant gene when AA was added, suggesting that all of the mutant enzymes were indeed active (Figure S12).

Because our aim was to understand how the ZmAAMT1 has such high specificity for AA in comparison to SA, we also included one additional ZmAAMT1 mutant, I274Q, based on the data from the CsSAMT Q263Y mutant (Figure 3; Table 1). The activity of the wild-type and each of the 13 mutant enzymes was determined *in vivo* by adding SA to the *E. coli* cultures that were expressing each gene, and extracts of the spent media were analyzed by GC–MS for MeSA. Three ZmAAMT1 mutants – C165S, Y246W, and L329M – generated 8.5-, 8-, and 2-fold more MeSA, respectively, relative to the wild-type enzyme when expressed *in vivo* (Figure 4c). We did not see increased MeSA generated by the other 10 mutants *in vivo* (Figure S13). Taken together, these results demonstrate that Cys165 and Leu329 also contribute to AA specificity in ZmAAMT1, since mutating these residues to a Ser and Met, respectively, increased activity with SA (Figure 4c). Because the L329M mutant has overall increased activity with AA *in vitro* and *in vivo*, this has implications for the production of MeAA in engineered organisms (Figure 4a,b) (Luo et al., 2019).

Structure–function-sequence evolution across AAMTs

To begin to understand the evolutionary relationship of the AA-using enzymes investigated here – the grape methyltransferases (4g02122, 4g02123, and 4g02169), the citrus

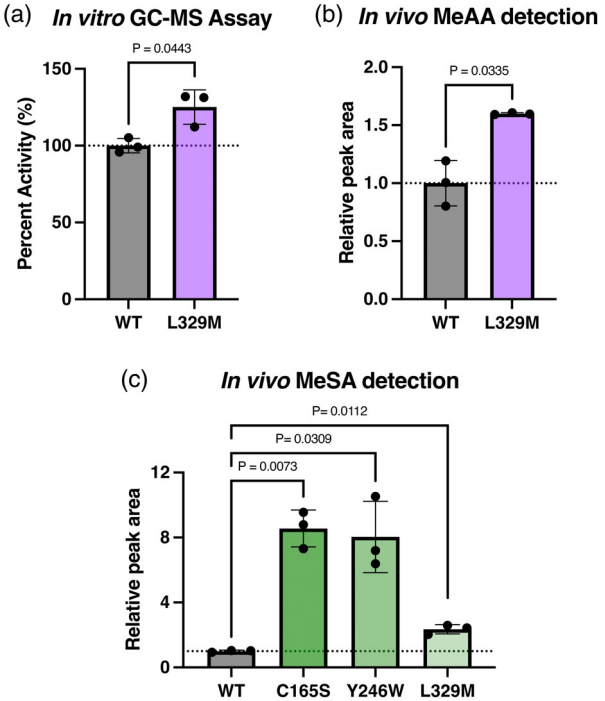

Figure 4. Identification of residues in the ZmAAMT1 active site that impart activity with methyl salicylate (MeSA).
(a) The increased activity of the L329M mutant compared to the wild-type ZmAAMT1 was confirmed by quantitative gas chromatography–mass spectrometry (GC–MS).
(b) Methyl anthranilate (MeAA) was compared in *Escherichia coli* cultures expressing *ZmAAMT1* or the *L329M* mutant, which was determined by GC–MS.
(c) MeSA was compared in *E. coli* cultures expressing *ZmAAMT1* or the *C165S*, *Y246W*, or *L329M* mutants, which was determined by GC–MS. For all points, $n = 3$; where error bars are not visible, the standard deviation is too small to visualize. *P*-values were calculated using a two-tailed Welch's *t*-test.

SAMT, and the maize AAMT1, a phylogeny was constructed (Figure S14). The CsSAMT and ZmAAMT1 have already been phylogenetically characterized, and the dendrogram generated here is consistent with previous analyses (Dubs et al., 2022; Huang et al., 2016; Köllner et al., 2010; Pollier et al., 2019). Of the grape enzymes, two (4g02122 and 4g02123) share an ancestor with each other and with other SAMTs, and because these two genes are clustered in close proximity on chromosome 4 and are active with either AA or SA, the AAMT and *N*-MeAAMT activity in these two *Vitis* genes may have evolved through gene duplication followed by neofunctionalization. Interestingly, the third grape enzyme, 4g02169, clustered with characterized jasmonic acid methyltransferases (JMTs). This was also true of the strawberry (*Fragaria* spp.) AAMT, which also has shared ancestry with JMTs (Pillet et al., 2017). When we assayed Vv4g02169 with jasmonic acid (JA), there was activity, although it was 5-fold lower than the enzyme's activity with AA (Figure 2a; Figure S15).

To connect protein structure and function to sequence evolution, we compared the active site residues that were investigated here across all of the methyltransferases in the phylogeny (Figure S14). In the CsSAMT active site, we identified four residues that are important for conferring AA activity: Gln263, Cys319, and Ala324 (Figure 5a; Table 1). Gln263 is conserved in Vv4g02122, Vv4g02123, and the soybean AAMT, but variable across the other functionally characterized AAMTs (Tyr in Vv4g02169; Ile in ZmAAMT1; Asn in the alfalfa AAMT) (Figure 5c; Figure S14). A notable trend is that enzymes that have a Gln in this position can all also methylate SA, but the AA-using enzymes that have a different residue have very little to no activity with SA (Table 1; Figure 2a) (Pollier et al., 2019). The CsSAMT Cys319 residue is a Leu in Vv4g02122 and 4g02123 and a Ser in Vv4g02169; introducing a polar Ser at this position in the CsSAMT increased overall activity and increased activity with AA, suggesting that this position may contribute to the high AA activity in Vv4g02169 (Figure 5c; Table 1). The CsSAMT A324M mutation increased AA activity twofold, and this mutant only had a detectable K_m value for AA. This Ala is conserved in almost all AA-using methyltransferases but is a conserved Met in the maize AAMTs and a Gln in Vv4g02169 (Figure 5c; Figure S14). Introducing a larger, nonpolar Met at this active site position may facilitate the positioning of the aromatic ring of AA, SA, and BA.

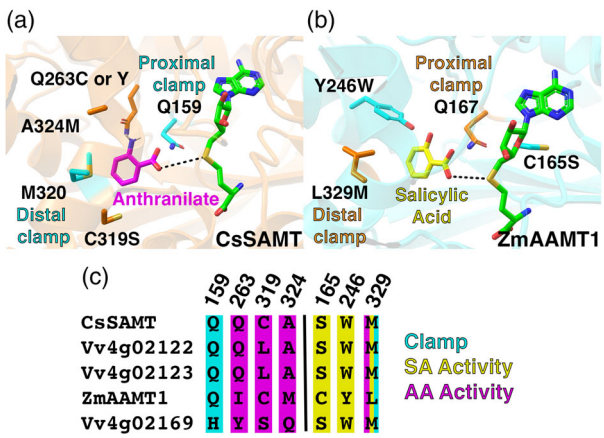

Figure 5. Connecting substrate specificity to protein structure.
(a) The *Citrus sinensis* SAMT active site with anthranilate (magenta) and SAH (green) bound. Four mutations at three residues (Q263C, Q263Y, C319S, and A324M) were important for conferring AA activity. Gln159 and Met320 (cyan) form a molecular clamp.
(b) The *Zea mays* AAMT1 active site with salicylic acid (yellow) and SAH (green) bound. Three mutations (C165S, Y246W, and L329M) increased activity with SA; L329M also increased activity with AA. Gln167 and Leu329 (orange) form a molecular clamp.
(c) Amino acid sequence alignment of the active site residues that conferred AA activity in CsSAMT (left of the black bar; numbers correspond to CsSAMT) or that conferred SA activity in ZmAAMT1 (right; numbers correspond to ZmAAMT1). AA, anthranilate; SA, salicylic acid.

In the maize AAMT1 active site, we identified two residues – in addition to Tyr246 that had been identified previously (Kollner et al., 2010) – that are important for conferring SA activity: Cys165 and Leu329 (Figures 4c and 5b). Cys165 is a polar Ser in almost all of the other AA and SA methyltransferases (Figure 5c; Figure S14). Having a polar residue at this position may aid in positioning acyl acid substrates for the methyl group transfer from SAM. The maize AAMT Leu329 (which corresponds to position 320 in the CsSAMT) is a nonpolar Met or Ile in the other AAMTs, so the fact that the conservative L329M mutation led to increased MeAA and MeSA production was surprising. Because Trp levels in maize are low (Kaur et al., 2020), having a Leu in position 329 that reduces AAMT1 activity suggests that there is weaker selective pressure for MeAA biosynthesis in maize (Bar-Even et al., 2011). Also, the reduced ZmAAMT1 activity may ensure that there is sufficient AA to support the biosynthesis of Trp, benzoxazinoids, and auxin hormones (Maeda & Dudareva, 2012).

Other investigations of active site residues in SAMTs have identified two Met residues that form a molecular clamp in the *C. breweri* SAMT to position the benzyl ring of SA in the active site (Zubieta et al., 2003). This clamp is formed by Gln159 and Met320 in CsSAMT; Gln167 and Leu329 in ZmAAMT1; Gln156 and Met314 in Vv4g02123; and His156 and Met316 in Vv4g02169 (Figure 5). The proximal clamp residue has also been implicated in substrate preference for SA versus BA, and others have found that having a Met at position 150 is a key determinant of SA substrate preference (Barkman et al., 2007; Dubs et al., 2022; Han et al., 2018). In our experiments, the proximal clamp residue seemed to matter less for determining AA substrate specificity, which is expected given that this site is ancestral in SAMT enzymes (Dubs et al., 2022). When the CsSAMT Gln159 was mutated to a His, activity was reduced with all three acyl acid substrates – SA, AA, and BA (Table 1). The distal clamp residue seemed to impact substrate specificity more. The ZmAAMT1 L329M mutant in effect introduces the same clamp residues (Gln and Met) that are found in the CsSAMT and Vv4g02123 active sites, both of which have high activity with SA (Table 1; Figure 2d,g). The fact that ZmAAMT1 L329M has higher activity overall further suggests that having the thioether moiety in the distal clamp position is important for AA and SA activity (Figure 4).

Overall, our findings, coupled with those from other SAM-dependent carboxy methyltransferases, highlight that there are multiple active site residues that confer substrate specificity. There is likely some context dependence as well, meaning that the combination of residues that make up the active site collectively impart specificity for AA versus other acyl acids. Additionally, we found residues outside the active site in the "Concord" 4g02123 that altered

activity, which was unanticipated (Figure 2e–g,i). As new AAMTs are discovered and more sequence data are available, it may become easier to predict which combinations of residues are required for AA activity.

Conclusions and future directions

Here, we identified two *V. vinifera* SAM-dependent methyltransferases (Vv4g02123 and Vv4g02169), as well as a "Concord" grape ortholog of 4g02123, that can generate the volatile MeAA (Table 1; Figure 2). Probing the molecular basis of AA recognition in a citrus SAMT led us to identify three key residues responsible for AA activity: Gln263, Cys319, and Ala324 (Table 1; Figure 5). Conversely, in the maize AAMT1, examining the basis of SA activity led us to identify two residues, Cys165 and Leu329, in addition to the previously identified Tyr246 (Kollner et al., 2010). MeAA has been under-sampled in plants, especially in below-ground tissues (Pollier et al., 2019). Since all plants synthesize AA as an intermediate in Trp biosynthesis (Li et al., 2023), there may be many more plant methyltransferases that can act on AA that remain to be discovered.

Because MeAA is commercially relevant, there is interest in using engineered microorganisms for MeAA production, as opposed to current practices that use non-renewable petroleum sources (Yadav & Krishnan, 1998). MeAA synthesized from yeast or bacteria is considered a natural flavor, and an engineered bacterium strain overexpressing the maize *AAMT1* gene generated 5.74 g L^{-1} of MeAA (Luo et al., 2019). The *Vitis* enzymes identified in our experiments may promote even higher yield in a synthetic biology platform. Identification of a DiMeAA-producing enzyme may also have implications for human health, as evidence suggests that DiMeAA has anti-nociceptive, anti-depression, and anti-anxiety effects in mice (Pinheiro et al., 2014; Radulovic et al., 2013). This is unsurprising considering a number of AA-derived alkaloids are bioactive (Shende et al., 2024). Additionally, identifying grape AAMTs has the potential to improve grape breeding to decrease MeAA levels in wine and eliminate the "foxy" dor. Our findings highlight the power of coupling existing "omics" data with characterizations of enzyme structure and function to reveal potential avenues to engineer plant volatile biosynthesis.

EXPERIMENTAL PROCEDURES

Protein visualization and molecular docking

Structural models of all proteins were obtained from AlphaFold (Jumper et al., 2021) (Uniprot IDs: CsSAMT: A0A1S8AD96; Vv4g02123: A0A438BRB9; Vv4g02169: D7SNV7; and ZmAAMT1: D9J0Z7), and AA was docked into each active site using AutoDock Vina (ver. 1.1.2) with a grid box of 40 × 40 × 40 Å and the exhaustiveness set to 8 (Forli et al., 2016; Trott & Olson, 2010). The results were visualized in PyMOL (ver. 2.5.7) (https://www.pymol.org/2/). Dimer complexes were generated using ColabFold v1.5.5 (Mirdita et al., 2022), and SAH was added to the dimers using AlphaFill (Hekkelman et al., 2023).

Site-directed mutagenesis

The wild-type amino acid sequences for CsSAMT (XP_006466836.1), ZmAAMT1 (D9J0Z8.1), Vv4g02122 (XP_002262759.2), Vv4g02123 (XP_002262676.1), Vv4g02169 (XP_002263459.1), and Vv12g00725 (XP_002267308.1) were used for codon-optimized gene synthesis (Data S1) and cloning into the *E. coli* pET28a expression vector by Twist Biosciences (South San Francisco, CA, USA). The wild-type plasmids were used as a template for site-directed mutagenesis PCR, and mutations were introduced using the QuikChange PCR method (Agilent, Santa Clara, CA, USA). Oligonucleotides were designed using PrimerX (https://www.bioinformatics.org/primerx/) or the Agilent QuikChange Primer Design tool (Table S1). The successful introduction of each mutation was determined by Sanger sequencing (Genewiz, South Plainfield, NJ, USA).

Protein expression and purification

Each construct was transformed into *E. coli* BL21 (DE3) cells (New England Biolabs, Ipswich, MA, USA). Cells were cultured in 1 L of Terrific broth until the A_{600nm} reached 0.6–0.8, at which time the incubator temperature was lowered to 16°C and protein expression was induced using 1 mM IPTG. After overnight incubation, cells were pelleted by centrifugation (5000 ***g***; 15 min) and resuspended in 40 ml of lysis buffer (50 mM Tris [pH 8.0], 500 mM NaCl, 20 mM imidazole, 10% glycerol, and 1% Tween-20). Following sonication, cell debris was removed by centrifugation (13 000 ***g***; 60 min) and the resulting lysate was passed over a Ni^{2+}-nitrilotriacetic acid column (1.5 × 12 cm) equilibrated in the lysis buffer. The column was then washed (50 mM Tris [pH 8.0], 500 mM NaCl, 20 mM imidazole, and 10% glycerol) and bound His-tagged protein eluted (50 mM Tris [pH 8.0], 500 mM NaCl, 250 mM imidazole, and 10% glycerol). Protein aliquots were stored at −80°C. Protein concentration was determined by the Bradford method (Bio-Rad, Hercules, CA, USA) with bovine serum albumin as the standard.

Luminescence kinetics assay

All *Citrus* and *Vitis* enzymes were assayed using the MTase-Glo™ methyltransferase assay (Promega, Madison, WI, USA) (Hsiao et al., 2016). A 4× reaction buffer was prepared so that the final concentrations in each well were 20 mM Tris (pH 8.0), 50 mM NaCl, 1 mM EDTA, 3 mM $MgCl_2$, 200 μg ml^{-1} bovine serum albumin, and 1 mM TCEP. The concentration of each protein was adjusted to 14–22 μg, and the wild-type and mutant enzymes were each assayed in triplicate with SAM (100 μM for CsSAMT and its mutants; 20 μM for 4g02123 from *V. vinifera* and its ortholog from "Concord"; 150 μM for Vv4g02122 and Vv4g02169) and 0–1 mM substrate with at least five concentrations of AA, SA, BA, or *N*-MeAA (Figure S16). The 20 μl reactions were initiated by the addition of substrates, and the reactions were incubated at 37°C for 30 min. Reactions were quenched by the addition of 5 μl of 0.5% trifluoroacetic acid before adding the 5 μl of 6× MTase-Glo reagent and subsequent 30 μl of MTase-Glo detection solution. Luminescence readings were measured using a BioTek Cytation 1 plate reader. The enzyme activity was calculated in terms of nmol of product per milligram of enzyme using a SAH standard curve ranging from 0 to 12 500 μM with five concentrations in between (n = 3) (Figure S1).

In vitro assays for MeAA detection

A 100 μl assay (100 mM HEPES [pH 7.5], 2 mM EDTA [pH 8.0], 10% glycerol, 25 μg of methyltransferase, and 1 mM AA or SA) was initiated by the addition of a final concentration of 2 mM SAM, and 1 ml of hexanes was overlaid on top of the reaction to trap the volatile products. The reaction mixture was then maintained at 37°C for 1 h, after which time the reactions were vortexed to quench the reaction. For quantitative analysis, 550 nM ethyl AA was added to the hexane as an internal standard for GC–MS analysis.

In vivo assay for MeAA and MeSA detection

Following the methods of Dubs and colleagues (Dubs et al., 2022), cultures of *E. coli* BL21 harboring the pET28a plasmid with the *ZmAAMT1* gene, the "Concord" ortholog of *4g02169*, or their mutants were grown in 50 ml of Terrific broth until the A_{600nm} reached 0.6–0.8, at which time the incubator temperature was lowered to 16°C and protein expression was induced using 1 mM IPTG. At the same time, SA or AA was added to the cultures at a final concentration of 200 μM. The following day, cells were pelleted (3500 ***g*** for 10 min), and 5 ml of hexanes were added to 45 ml of the spent media. After vortex mixing and centrifuging (3500 ***g*** for 5 min), the hexane layer was analyzed by GC–MS.

GC–MS analysis

The ZmAAMT1 samples were analyzed using a 7820A gas chromatograph system coupled to a 5977B mass selective detector (Agilent Technologies, Santa Clara, CA, USA). Data were acquired and processed using MassHunter Agilent Technologies™ Software. The selected ion monitoring mode was used to search for specific ions to identify and quantify *O*-methyl anthranilate (*m/z* of 92, 119, and 151) and *O*-ethyl anthranilate and dimethyl anthranilate (*m/z* of 92, 119, 151, and 165), and external standards of pure compounds were included with each run (MilliporeSigma, St. Louis, MO, USA). Each ion was measured with a dwell time of 100 msec. A solvent delay for the MS of 2.0 min was used. A splitless injection volume of 1 μl was injected onto an HP-5 column with 5% phenyl methylpolysiloxane stationary phase (Agilent) with dimensions of 30 m × 0.25 mm × 0.25 μm. Helium was used as the carrier gas with a flow rate of 1.2 ml min^{-1}. The injection port was set at 280°C with a purge flow of 50 ml min^{-1} at 0.4 min. For the ZmAAMT1 *in vitro* assay samples, the oven temperature was initially set at 110°C, held at that temperature for 2 min and then increased at a rate of 30°C min^{-1} until 270°C, where it was held for 2 min; total run time was 9.33 min. For the *in vivo E. coli* extracts and the *in vitro* grape assays, the oven temperature was initially set at 60°C, held for 2 min and then increased at a rate of 30°C min^{-1} until 300°C, where it was held for 2 min; total run time was 12 min. Data were acquired and processed using MassHunter Agilent Technologies™ Software. For MeAA quantification produced by ZmAAMT1 *in vitro*, the limit of detection and limit of quantification were determined, and a calibration curve was generated using triplicate values from 0 to 2000 nM for MeAA and the internal standard EtAA (Figure S11) (Hubaux & Vos, 1970). The products of the *Vitis* enzymes were confirmed *in vitro* using the same method on a 7890B GC coupled to a 7000C triple-quadrupole mass spectrometer (Agilent Technologies).

Assay for ZmAAMT1 activity using ^{14}C-SAM

The assay followed a published method (Kollner et al., 2010), and each 100 μl reaction contained 25 μg of methyltransferase buffered with 100 mM HEPES (pH 7.5), 2 mM EDTA (pH 8.0), and 10% glycerol. AA and SA were tested at a final concentration of 1 mM, and the reactions were initiated by the addition of 3 μl of 52.6 mCi $mmol^{-1}$ S-[methyl-^{14}C]adenosyl-L-methionine (PerkinElmer, Waltham, MA, USA). The reaction was overlaid with 1 ml of pentane and incubated at 37°C for 1 h. The reactions were quenched by vortexing, and the pentane layer was mixed 1:5 (v/v) with Scintiverse BD Biodegradable LSC cocktail (Fisher Scientific, Hampton, NH, USA). The scintillation vials were read in a Beckman LS 6500 multiple-purpose scintillation counter (96.38% efficiency). Counts per minute were used to calculate the activity in nmol mg^{-1} of protein.

Phylogenetic analysis

Homologous sequences and an outgroup were selected from SAMT and JMT clades based on comprehensive characterization and phylogenetic analyses of plant SABATH methyltransferases (Dubs et al., 2022; Koeduka et al., 2020; Kollner et al., 2010). Amino acid sequences were aligned using MAFFT version 7 (Katoh & Standley, 2013). Protein phylogenies were inferred using the IQ-TREE web server with default parameters and 10 000 ultrafast bootstrap replicates (Hoang et al., 2017; Kalyaanamoorthy et al., 2017; Nguyen et al., 2014). The best-fit model according to Bayesian Information Criterion was the JTT model with a discrete Gamma model with four rate categories (Jones et al., 1992; Yang, 1994). The dendrogram was visualized using FigTree (version 1.4.4).

AUTHOR CONTRIBUTIONS

NC, MMD, MAF, CKH, HT, and APW designed the research; MMD, MAF, CF, CKH, HT, and APW performed the research; all authors contributed to data analysis; CKH wrote the paper with all authors providing editorial input.

ACKNOWLEDGMENTS

We thank Holland lab members for their feedback on this work, as well as Drs. Lucas Busta, Tara Enders, and Thomas Smith for helpful conversations. This research was supported by funds from Williams College and the U.S. National Science Foundation (MCB-2214883 to C.K.H.), and H.T. was funded by the American Society of Plant Biologists through a Summer Undergraduate Research Fellowship. Portions of the mass spectral data were obtained at the University of Massachusetts Mass Spectrometry Core Facility, RRID:SCR_019063.

CONFLICT OF INTEREST

The authors declare no competing interests.

DATA AVAILABILITY STATEMENT

All relevant data can be found within the manuscript and its supporting materials.

SUPPORTING INFORMATION

Additional Supporting Information may be found in the online version of this article.

Figure S1. Kinetic plots of the activities of *Vitis vinifera* (Vv) 4g02122, 4g02123, and "Concord" ortholog of 4g02123 with BA or SA.

Figure S2. GC–MS data confirms that 4g02123 from "Concord" and wine grapes (Vv) synthesizes methyl anthranilate (MeAA) *in vitro*.

Figure S3. GC–MS data confirms that 4g02123 from "Concord" and wine grapes (Vv) synthesizes dimethyl anthranilate (DiMeAA) *in vitro*.

Figure S4. Promoter sequence comparisons for *Vitis vinifera* Vv4g02123 and its orthologs in *Vitis labrusca* and "Concord" grapes.

Figure S5. Promoter sequence comparisons for *Vitis vinifera* Vv4g02169 and its orthologs in *Vitis labrusca* and "Concord" grapes.

Figure S6. Coding sequence alignment of *Vitis vinifera* Vv4g02123 and its orthologs in *Vitis labrusca* and "Concord" grapes.

Figure S7. Coding sequence alignment of *Vitis vinifera* Vv4g02169 and its orthologs in *Vitis labrusca* and "Concord" grapes.

Figure S8. Michaelis–Menten plots of *Citrus sinensis* (Cs) SAMT activity with SA, AA, or BA.

Figure S9. Ratio of activity with AA relative to SA for the *Citrus sinensis* SAMT.

Figure S10. Percent activity of ZmAAMT1 mutants with 1 mM anthranilate or 1 mM salicylic acid relative to wild type, which was determined using ^{14}C-SAM.

Figure S11. GC–MS data for *in vitro* MeAA quantification for the wild-type ZmAAMT1 enzyme and the L329M mutant.

Figure S12. GC–MS chromatograms for *in vivo* ZmAAMT1 MeAA detection.

Figure S13. GC–MS chromatograms for *in vivo* ZmAAMT1 MeSA detection.

Figure S14. Dendrogram of plant acyl acid methyltransferases.

Figure S15. Jasmonic acid (JA) activity in the Vv4g02169 enzyme.

Figure S16. SAM kinetics plots of CsSAMT with saturating salicylic acid and Vv4g02122, Vv4g02123, and Vv4g02169 with saturating anthranilate.

Table S1. List of primers used for site-directed mutagenesis.

Data S1. Codon-optimized gene sequences of *AAMTs* and *SAMTs*.

REFERENCES

Avery, M.L., **Decker, D.G.**, **Humphrey, J.S.**, **Aronov, E.**, **Linscombe, S.D.** & **Way, M.** (1995) Methyl anthranilate as a rice seed treatment to deter birds. *The Journal of Wildlife Management*, **59**, 50–56.

Azam, M., **Song, M.**, **Fan, F.**, **Zhang, B.**, **Xu, Y.**, **Xu, C.** ***et al.*** (2013) Comparative analysis of flower volatiles from nine citrus at three blooming stages. *International Journal of Molecular Sciences*, **14**, 22346–22367.

Baldwin, I.T. (2010) Plant volatiles. *Current Biology*, **20**, R392–R397.

Bar-Even, A., **Noor, E.**, **Savir, Y.**, **Liebermeister, W.**, **Davidi, D.**, **Tawfik, D.S.** ***et al.*** (2011) The moderately efficient enzyme: evolutionary and physicochemical trends shaping enzyme parameters. *Biochemistry*, **50**, 4402–4410.

Barkman, T.J., **Martins, T.R.**, **Sutton, E.** & **Stout, J.T.** (2007) Positive selection for single amino acid change promotes substrate discrimination of a plant volatile-producing enzyme. *Molecular Biology and Evolution*, **24**, 1320–1329.

Bracker, L.B., **Gong, X.**, **Schmid, C.**, **Dawid, C.**, **Ulrich, D.**, **Phung, T.** ***et al.*** (2020) A strawberry accession with elevated methyl anthranilate fruit concentration is naturally resistant to the pest fly *Drosophila suzukii*. *PLoS One*, **15**, e0234040.

Dubs, N.M., **Davis, B.R.**, **de Brito, V.**, **Colebrook, K.C.**, **Tiefel, I.J.**, **Nakayama, M.B.** ***et al.*** (2022) A collaborative classroom investigation of the evolution of SABATH Methyltransferase substrate preference shifts over 120 my of flowering plant history. *Molecular Biology and Evolution*, **39**, msac007.

Dudareva, N., **Negre, F.**, **Nagegowda, D.A.** & **Orlova, I.** (2006) Plant volatiles: recent advances and future perspectives. *Critical Reviews in Plant Sciences*, **25**, 417–440.

Dudareva, N., **Pichersky, E.** & **Gershenzon, J.** (2004) Biochemistry of plant volatiles. *Plant Physiology*, **135**, 1893–1902.

Effmert, U., **Saschenbrecker, S.**, **Ross, J.**, **Negre, F.**, **Fraser, C.M.**, **Noel, J.P.** ***et al.*** (2005) Floral benzenoid carboxyl methyltransferases: from in vitro to in planta function. *Phytochemistry*, **66**, 1211–1230.

Forli, S., **Huey, R.**, **Pique, M.E.**, **Sanner, M.F.**, **Goodsell, D.S.** & **Olson, A.J.** (2016) Computational protein-ligand docking and virtual drug screening with the AutoDock suite. *Nature Protocols*, **11**, 905–919.

Gong, Q., **Wang, Y.**, **He, L.**, **Huang, F.**, **Zhang, D.**, **Wang, Y.** ***et al.*** (2023) Molecular basis of methyl-salicylate-mediated plant airborne defence. *Nature*, **622**, 139–148.

Gonzalez-Mas, M.C., **Rambla, J.L.**, **Lopez-Gresa, M.P.**, **Blazquez, M.A.** & **Granell, A.** (2019) Volatile compounds in citrus essential oils: a comprehensive review. *Frontiers in Plant Science*, **10**, 12.

Han, X.M., **Yang, Q.**, **Liu, Y.J.**, **Yang, Z.L.**, **Wang, X.R.**, **Zeng, Q.Y.** ***et al.*** (2018) Evolution and function of the *Populus* SABATH family reveal that a single amino acid change results in a substrate switch. *Plant & Cell Physiology*, **59**, 392–403.

Hekkelman, M.L., **de Vries, I.**, **Joosten, R.P.** & **Perrakis, A.** (2023) AlphaFill: enriching AlphaFold models with ligands and cofactors. *Nature Methods*, **20**, 205–213.

Hoang, D.T., **Chernomor, O.**, **von Haeseler, A.**, **Minh, B.Q.** & **Vinh, L.S.** (2017) UFBoot2: improving the ultrafast bootstrap approximation. *Molecular Biology and Evolution*, **35**, 518–522.

Hsiao, K., **Zegzouti, H.** & **Goueli, S.A.** (2016) Methyltransferase-Glo: a universal, bioluminescent and homogenous assay for monitoring all classes of methyltransferases. *Epigenomics*, **8**, 321–339.

Huang, R., **O'Donnell, A.J.**, **Barboline, J.J.** & **Barkman, T.J.** (2016) Convergent evolution of caffeine in plants by co-option of exapted ancestral enzymes. *Proceedings of the National Academy of Sciences of the United States of America*, **113**, 10613–10618.

Hubaux, A. & **Vos, G.** (1970) Decision and detection limits for calibration curves. *Analytical Chemistry*, **42**, 849–855.

Jones, D.T., **Taylor, W.R.** & **Thornton, J.M.** (1992) The rapid generation of mutation data matrices from protein sequences. *Bioinformatics*, **8**, 275–282.

Jumper, J., **Evans, R.**, **Pritzel, A.**, **Green, T.**, **Figurnov, M.**, **Ronneberger, O.** ***et al.*** (2021) Highly accurate protein structure prediction with alphafold. *Nature*, **596**, 583–589.

Kalyaanamoorthy, S., **Minh, B.Q.**, **Wong, T.K.F.**, **von Haeseler, A.** & **Jermiin, L.S.** (2017) ModelFinder: fast model selection for accurate phylogenetic estimates. *Nature Methods*, **14**, 587–589.

Katoh, K. & **Standley, D.M.** (2013) MAFFT multiple sequence alignment software version 7: improvements in performance and usability. *Molecular Biology and Evolution*, **30**, 772–780.

Kaur, R., **Kaur, G.**, **Vikal, Y.**, **Gill, G.K.**, **Sharma, S.**, **Singh, J.** ***et al.*** (2020) Genetic enhancement of essential amino acids for nutritional enrichment of maize protein quality through marker assisted selection. *Physiology and Molecular Biology of Plants*, **26**, 2243–2254.

Knudsen, J.T., **Eriksson, R.**, **Gershenzon, J.** & **Ståhl, B.** (2006) Diversity and distribution of floral scent. *The Botanical Review*, **72**, 1–120.

Koeduka, T., **Suzuki, H.**, **Taguchi, G.** & **Matsui, K.** (2020) Biochemical characterization of the jasmonic acid methyltransferase gene from wasabi (*Eutrema japonicum*). *Plant Biotechnology (Tokyo)*, **37**, 389–392.

Kollner, T.G., **Lenk, C.**, **Zhao, N.**, **Seidl-Adams, I.**, **Gershenzon, J.**, **Chen, F.** ***et al.*** (2010) Herbivore-induced SABATH methyltransferases of maize that methylate anthranilic acid using s-adenosyl-L-methionine. *Plant Physiology*, **153**, 1795–1807.

Li, M., **Tadfie, H.**, **Darnell, C.G.** & **Holland, C.K.** (2023) Biochemical investigation of the tryptophan biosynthetic enzyme anthranilate phosphoribosyltransferase in plants. *Journal of Biological Chemistry*, **299**, 105197.

Lin, J., **Massonnet, M.** & **Cantu, D.** (2019) The genetic basis of grape and wine aroma. *Horticulture Research*, **6**, 81.

Lin, J., **Mazarei, M.**, **Zhao, N.**, **Zhu, J.J.**, **Zhuang, X.**, **Liu, W.** ***et al.*** (2013) Overexpression of a soybean salicylic acid methyltransferase gene confers resistance to soybean cyst nematode. *Plant Biotechnology Journal*, **11**, 1135–1145.

Luo, Z.W., **Cho, J.S.** & **Lee, S.Y.** (2019) Microbial production of methyl anthranilate, a grape flavor compound. *Proceedings of the National Academy of Sciences of the United States of America*, **116**, 10749–10756.

Maeda, H. & **Dudareva, N.** (2012) The shikimate pathway and aromatic amino acid biosynthesis in plants. *Annual Review of Plant Biology*, **63**, 73–105.

Mann, R.S., **Ali, J.G.**, **Hermann, S.L.**, **Tiwari, S.**, **Pelz-Stelinski, K.S.**, **Alborn, H.T.** ***et al.*** (2012) Induced release of a plant-defense volatile 'deceptively' attracts insect vectors to plants infected with a bacterial pathogen. *PLoS Pathogens*, **8**, e1002610.

Mason, J.R., **Adams, M.A.** & **Clark, L.** (1989) Anthranilate repellency to starlings: chemical correlates and sensory perception. *The Journal of Wildlife Management*, **53**, 55–64.

Mikiciuk, G., **Chełpiński, P.**, **Mikiciuk, M.**, **Możdżer, E.** & **Telesiński, A.** (2021) The effect of methyl anthranilate-based repellent on chemical composition and selected physiological parameters of sweet cherry (*Prunus avium* L.). *Agronomy*, **11**, 256.

Mirdita, M., **Schütze, K.**, **Moriwaki, Y.**, **Heo, L.**, **Ovchinnikov, S.** & **Steinegger, M.** (2022) ColabFold: making protein folding accessible to all. *Nature Methods*, **19**, 679–682.

Nguyen, L.-T., **Schmidt, H.A.**, **von Haeseler, A.** & **Minh, B.Q.** (2014) IQ-TREE: a fast and effective stochastic algorithm for estimating maximum-likelihood phylogenies. *Molecular Biology and Evolution*, **32**, 268–274.

Pillet, J., **Chambers, A.H.**, **Barbey, C.**, **Bao, Z.**, **Plotto, A.**, **Bai, J.** ***et al.*** (2017) Identification of a methyltransferase catalyzing the final step of methyl anthranilate synthesis in cultivated strawberry. *BMC Plant Biology*, **17**, 147.

Pinheiro, M.M.G., **Radulović, N.S.**, **Miltojević, A.B.**, **Boylan, F.** & **Fernandes, P.D.** (2014) Antinociceptive esters of N-methylanthranilic acid: mechanism of action in heat-mediated pain. *European Journal of Pharmacology*, **727**, 106–114.

Pollier, J., **De Geyter, N.**, **Moses, T.**, **Boachon, B.**, **Franco-Zorrilla, J.M.**, **Bai, Y.** ***et al.*** (2019) The MYB transcription factor emission of methyl anthranilate 1 stimulates emission of methyl anthranilate from Medicago truncatula hairy roots. *The Plant Journal*, **99**, 637–654.

Radulovic, N.S., **Miltojevic, A.B.**, **Randjelovic, P.J.**, **Stojanovic, N.M.** & **Boylan, F.** (2013) Effects of methyl and isopropyl N-methylanthranilates from *Choisya ternata* Kunth (Rutaceae) on experimental anxiety and depression in mice. *Phytotherapy Research*, **27**, 1334–1338.

Rohde, B., **Hans, J.**, **Martens, S.**, **Baumert, A.**, **Hunziker, P.** & **Matern, U.** (2008) Anthranilate N-methyltransferase, a branch-point enzyme of acridone biosynthesis. *The Plant Journal*, **53**, 541–553.

Sawler, J., **Reisch, B.**, **Aradhya, M.K.**, **Prins, B.**, **Zhong, G.-Y.**, **Schwaninger, H.** ***et al.*** (2013) Genomics assisted ancestry deconvolution in grape. *PLoS One*, **8**, e80791.

Schuman, M.C. (2023) Where, when, and why do Plant volatiles mediate ecological signaling? The answer is blowing in the wind. *Annual Review of Plant Biology*, **74**, 609–633.

Shende, V.V., **Bauman, K.D.** & **Moore, B.S.** (2024) The shikimate pathway: gateway to metabolic diversity. *Natural Product Reports*, **41**, 604–648.

Simpson, M., **Gurr, G.M.**, **Simmons, A.T.**, **Wratten, S.D.**, **James, D.G.**, **Leeson, G.** ***et al.*** (2011) Insect attraction to synthetic herbivore-induced plant volatile-treated field crops. *Agricultural and Forest Entomology*, **13**, 45–57.

Sun, Q., **Gates, M.J.**, **Lavin, E.H.**, **Acree, T.E.** & **Sacks, G.L.** (2011) Comparison of odor-active compounds in grapes and wines from Vitis vinifera and non-foxy American grape species. *Journal of Agricultural and Food Chemistry*, **59**, 10657–10664.

Trott, O. & **Olson, A.J.** (2010) AutoDock Vina: improving the speed and accuracy of docking with a new scoring function, efficient optimization, and multithreading. *Journal of Computational Chemistry*, **31**, 455–461.

Turlings, T.C., **Tumlinson, J.H.** & **Lewis, W.J.** (1990) Exploitation of herbivore-induced plant odors by host-seeking parasitic wasps. *Science*, **250**, 1251–1253.

von Merey, G.E., **Veyrat, N.**, **D'Alessandro, M.** & **Turlings, T.C.** (2013) Herbivore-induced maize leaf volatiles affect attraction and feeding behavior of *Spodoptera littoralis* caterpillars. *Frontiers in Plant Science*, **4**, 209.

Wang, J. & **De Luca, V.** (2005) The biosynthesis and regulation of biosynthesis of Concord grape fruit esters, including 'foxy' methylanthranilate. *The Plant Journal*, **44**, 606–619.

Westfall, C.S., **Muehler, A.M.** & **Jez, J.M.** (2013) Enzyme action in the regulation of plant hormone responses. *The Journal of Biological Chemistry*, **288**, 19304–19311.

Yadav, G.D. & **Krishnan, M.S.** (1998) An ecofriendly catalytic route for the preparation of perfumery grade methyl anthranilate from anthranilic acid and methanol. *Organic Process Research & Development*, **2**, 86–95.

Yang, Y., **Cuenca, J.**, **Wang, N.**, **Liang, Z.**, **Sun, H.**, **Gutierrez, B.** ***et al.*** (2020) A key 'foxy' aroma gene is regulated by homology-induced promoter indels in the iconic juice grape 'Concord'. *Horticulture Research*, **7**, 67.

Yang, Z. (1994) Maximum likelihood phylogenetic estimation from DNA sequences with variable rates over sites: approximate methods. *Journal of Molecular Evolution*, **39**, 306–314.

Zubieta, C., **Ross, J.R.**, **Koscheski, P.**, **Yang, Y.**, **Pichersky, E.** & **Noel, J.P.** (2003) Structural basis for substrate recognition in the salicylic acid carboxyl methyltransferase family. *The Plant Cell*, **15**, 1704–1716.